 DOI: 10.30420/566262107

Large-area Bonding with LMEE: Suppression of the Degradation of the Junction-to-Water Thermal Resistance in Power Modules

Yo Mochizuki[1], Takukazu Otsuka[1], Navid Kazem[2], Dylan Shah[2] and Ken Nakahara[1]

[1]ROHM Co., Ltd., Japan
[2]Arieca Inc., USA

Corresponding author: Yo Mochizuki, yo.mochizuki@rohm.co.jp
Speaker: Yo Mochizuki, yo.mochizuki@rohm.co.jp

Abstract

This paper investigates the junction-to-water thermal resistance (R_{th}) durability of power modules (PMs) during the thermal shock test (TST), in which the PMs were subjected to the thermal cycle from −40°C to 125°C with dwell time 20 min for up to 1000 cycles. The PMs contained silicon carbide power devices, and were bonded to a water cooler by using liquid metal embedded elastomers (LMEE). The bonding was performed at 150°C for 30 minutes under a pressure of 0.1 MPa. The R_{th} showed no significant degradation during the TST. This indicates that LMEE is a good candidate as a bonding material for PM-and-cooler assembly for enhancing its durability.

1 Introduction

Power modules (PMs) with high power density are highly anticipated for use in power conversion systems, such as those installed in electric vehicles (EVs). Power loss in the conversion inevitably generates heat and then the thermal resistance (R_{th}) plays a key role in maintaining system operations. The heat generated in such PMs is typically dissipated by a water cooler bonded to the PMs. Thermal interface material (TIM) is widely used for this bond, and thermal grease has typified such material [1]. However, the thermal conductivity (k) of commercial thermal grease is typically about 4 W/mK at maximum, which worsens the total R_{th} of PMs. In addition, a problem has been reported that grease is easily pumped out during the operation of PMs [2]. Thus, sintered silver (s-Ag) bonding has been actively studied due to its high k and high melting point [3,4]. However, the maximum bonding area is limited to approximately 10×10 mm because many cracks are easily induced by thermal stress [4].

The authors propose liquid metal embedded elastomers (LMEE) as a candidate for TIM to solve the above problems. LMEE consists of a silicone elastomer embedded with liquid phase eutectic gallium indium. LMEE typically exhibits a fracture strain of 300%, k = 10 W/mK, and a Young's modulus of 0.4 MPa. In particular, this higher k than that of grease is likely to be attractive for achieving low R_{th} [5].

In this study, the R_{th} of a LMEE-bonded PM and water cooler assembly was observed during a thermal shock test (TST). The next section describes the experimental setup in detail. In the last section, we show the effectiveness of LMEE on the R_{th} durability.

2 Experimental methodology

Fig. 1 shows a cross-sectional sketch of the structure used in this study. "SiC" denotes silicon carbide, and "AMB" denotes a silicon nitride ceramic plate sandwiched with copper plates. SiC chips were bonded onto the AMB at 300 °C by using s-Ag (average diameter: 18 nm) for 10 minutes under a pressure of 30 MPa (CYPM-200, manufactured by SHINTOKOGIO, LTD, Aichi, Japan). Lead flames were bonded onto the top surface of the AMB by soldering with Sn-Ag3%-Cu0.5% system at 230 °C in the formic acid reduction atmosphere. Then, wedge Al wire bonding was performed between the flame and the SiC chips surfaces in an air atmosphere. These bonded bodies were molded with epoxy resin, and finally the molded bodies, each representing a PM in actual use, were bonded to water coolers with s-Ag and LMEE. For s-Ag

ISBN 978-3-8007-6262-0

bonding, 210°C for 10 minutes under a pressure of 20 MPa was used, while for LMEE bonding, 150°C for 30 minutes under a pressure of 0.1 MPa was used. The dimensions of the bodies are listed in Table 1.

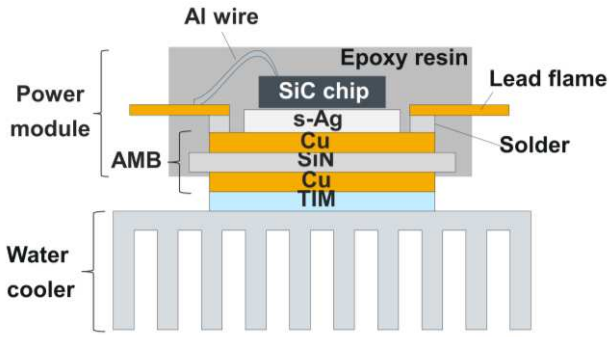

Fig. 1 Cross-sectional schematic view of an evaluated assemble.

	Width	Length	Thickness
SiC chip	4.8	4.8	0.35
s-Ag	7	7	0.05
AMB	30	42	1.12
TIM	30	42	0.05(LMEE) 0.15(s-Ag)
Water cooler	142	59	13

Table 1 The dimensions of each part（Unit: mm)

Figs. 2 show the cross-sectional images of the material interfaces in an assembled structure. Figs. 2 (a) and (b) are the scanning electron micrography (SEM) images of a s-Ag layer, while Figs (c) and (d) are optical microscope images. SEM could not be used to charge up the LMEE. The s-Ag layer shows a porosity of ρ = 16.5%, determined from the binarized image of Fig. 2 (b).

The assemblies were placed in a commercial chamber (TSA41-EL-A, manufactured by Espec, Osaka, Japan), and the TST cycling was from −40°C to 125°C maintaining 30 minutes at each temperature for up to 1000 cycles. R_{th} was evaluated at TST 100-cycle intervals by transition thermal resistance measurement (A07M355, manufactured by Coper Electronics Co., Ltd., Kanagawa, Japan).

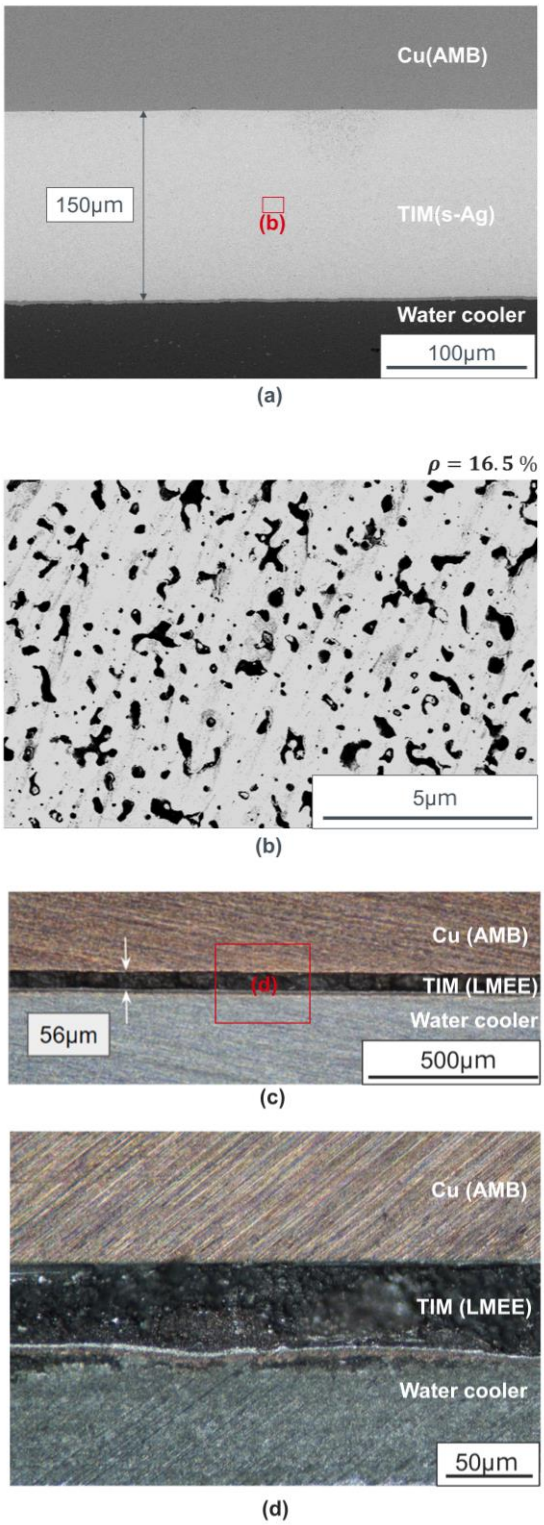

Fig. 2 Typical cross-sectional images of an assembled structure. (a): Overall picture and (b): microstructure of s-Ag observed with SEM. (c):Overall picture and (d): magnified picture of LMEE with an optical microscope.

3 Results & Discussion

Fig. 3 (a) shows the R_{th} measurement results at every 100 cycles of the TST. The vertical axis represents the increase rate of R_{th}, r_{th}, which is defined by the measured increase of R_{th} divided by the initial R_{th}. The initial R_{th} value of s-Ag and LMEE was almost identical, suggesting that LMEE has almost the same heat dissipation capacity as s-Ag, but r_{th} completely differed between these two materials. For s-Ag, as shown in Fig. 3 (a), r_{th} jumps up by about 10% just after 100 cycles of TST, and reaches 35% after 300 cycles of TST. This durability is not satisfied at all with the requirement on the R_{th} failure requirement in the EV market, i.e. 20% [6]. In stark contrast, however, the r_{th} for LMEE is approximately 4.1% even after 1000 cycles of TST. This means that LMEE has the excellent capacity as TIM to meet the requirement on the R_{th} failure requirement in the EV market.

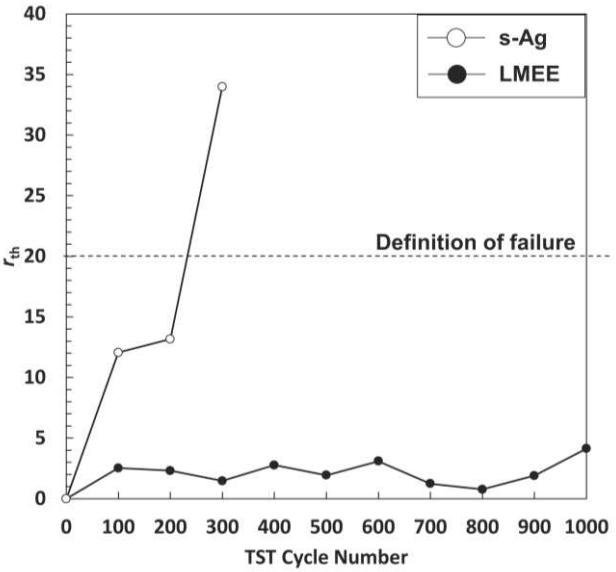

Fig. 3 (a) R_{th} measurement results during the TST.

Fig. 3 (b) shows the scanning acoustic tomography (SAT) image of s-Ag detected at bonded area after 300 cycles of TST (IS-350, manufactured by Insight k.k. Co., Ltd., Tokyo, Japan). The SAT image was obtained using an ultrasonic probe with 25 MHz. In the SAT image, a black-colored area shows bonded, while white and pale gray color means delamination. Therefore, the delamination was considered to increase r_{th} of s-Ag shown in Fig. 3 (a).

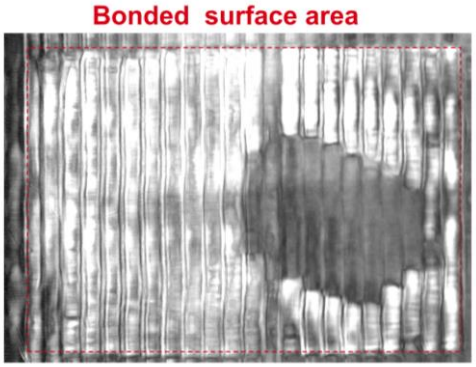

Fig. 3 (b) SAT image of s-Ag at bonded area after 300 cycles of TST. Red dash-square is bonded surface area.

Finite element analysis (FEA) was conducted to understand the out-of-plane deformation distribution, using software, FEMTET, in which simulation a cyclic temperature between -40 °C and 125 °C was set to the ambient atmosphere as a driving force of induced stress. The material characteristic values used for the FEA are listed in Table 2. In LMEE, elastic behavior was considered [5], In s-Ag the elastic-plastic behavior, as shown Fig. 4 [7].

Material	Young's Modulus (GPa)	Poison's Ratio	CTE ($\times 10^{-6}$)
Epoxy	15	0.3	12
SiC	412	0.17	3.0
Cu	118	0.35	16.8
Si_3N_4	300	0.3	2.7
s-Ag		0.35	19.5
LMEE	0.4	0.5	33
Al	68.5	0.34	23.1

Table 2 Material mechanical properties used in FEA. Young's Modulus of the s-Ag shown in Fig. 4.

ISBN 978-3-8007-6262-0

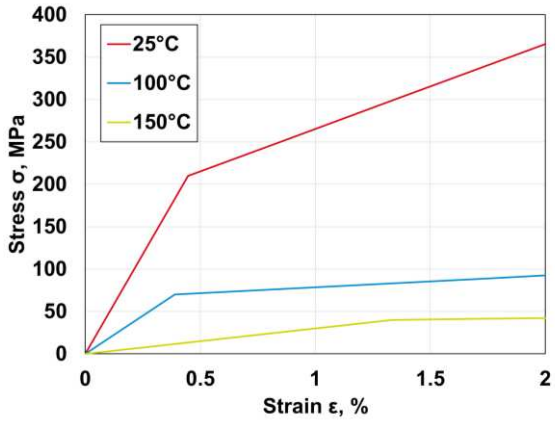

Fig. 4 *S-S* curves for each temperature with s-Ag [7] in FEA.

Figs. 5 depicts the FEA results for high (150 °C) and low (-40 °C) temperatures. The displacement diagram in FEA is the vertical axis component, shown as figures multiplied by 30. The s-Ag deforms more than 100 μm with temperature change, as shown Fig. 5 (b). In contrast, The LMEE only deforms less than 10 μm, as shown Fig 5 (c). Therefore, the s-Ag is considered to have degradation because of its greater displacement than LMEE.

FEA model

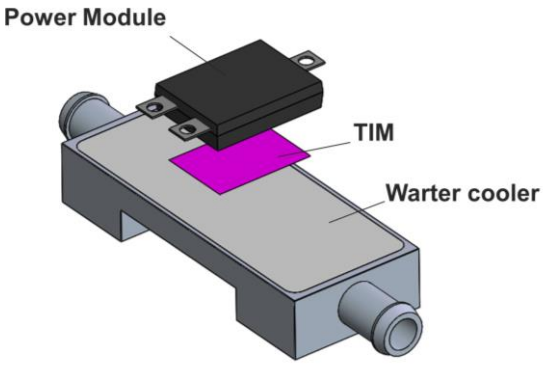

Fig. 5 (a) simulation model in FEA.

High temperature (150 °C)

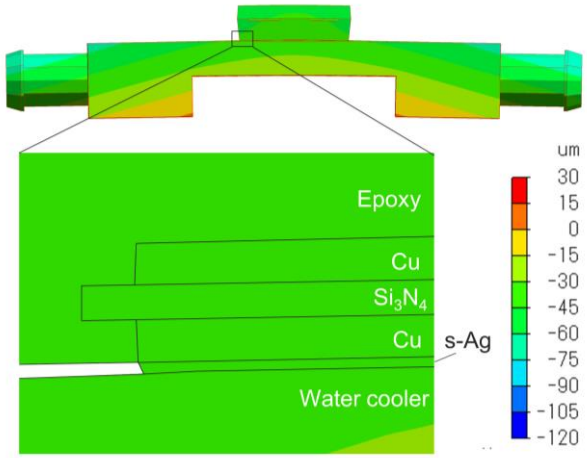

Low temperature (-40 °C)

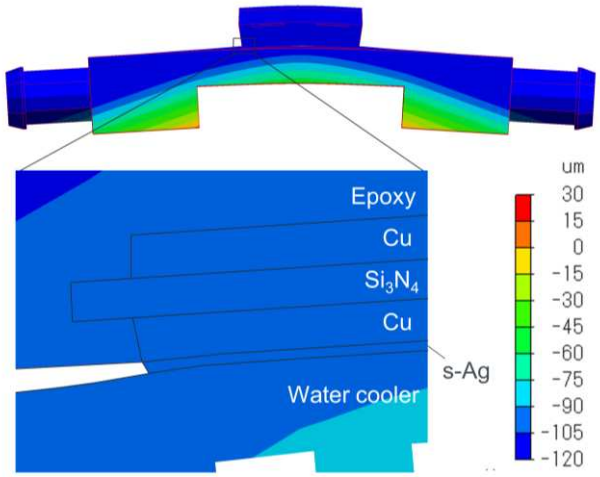

Fig. 5 (b) The out-of-plane deformation distribution with s-Ag in FEA.

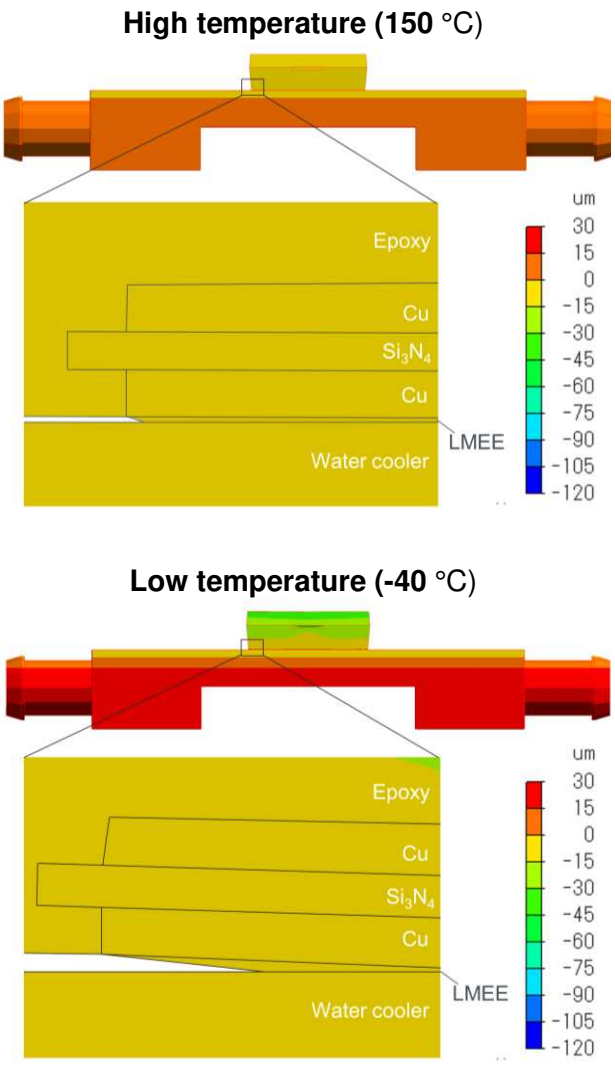

Fig. 5 (c) The out-of-plane deformation distribution with LMEE in FEA.

As for our future work, TST is not the only reliability test in the EV market, and accordingly we will conduct vibration tests, high-temperature storage tests, and humidity tests to verify LMEE's reliability potential.

References

[1] N. S. Goel et al., "Technical review of characterization methods for thermal interface Materials (TIM)," Intersociety Conference on Thermal and Thermomechanical Phenomena in Electronic Systems, May 2008.

[2] F. Sarvar, D. C. Whalley, and P. P. Conway, "Thermal Interface Materials - A Review of the State of the Art," Electronic Systemintegration Technology Conference, Sep, 2006, doi: 10.1109/ESTC.2006.280178.

[3] K. Wakamoto, T. Otsuka, K. Nakahara, V. Mugilgeethan, R. Matsumoto, and T. Namazu, "Degradation Mechanism of Silver Sintering Die Attach Based on Thermal and Mechanical Reliability Testing," IEEE Transactions on Components, Packaging and Manufacturing Technology, vol. 13, pp.197-210, Feb, 2023, doi: 10.1109/TCPMT.2023.3242423.

[4] P. Peng, A. Hu, A. P. Gerlich, G. Zou, L. Liu, and Y. N. Zhou, "Joining of Silver Nanomaterials at Low Temperatures: Processes, Properties, and Applications," ACS Appl Mater Interfaces, vol. 7, no. 23, pp. 1259712618, Jun. 2015

[5] W. Li, S. Liu, C. Lou, M. Sang, X. Gong, K. Leung, and S. Xuan "Magneto-induced self-stratifying liquid metal-elastomer composites with high thermal conductivity for soft actuator" Li et al., Cell Reports Physical Science, vol. 4, no. 1, p. 101209, Jan. 2023, doi: https://doi.org/10.1016/j.xcrp.2022.101209.

[6] "Qualification of Power Modules for Use in Power Electronics Converter Units in Motor Vehicles" EPCE Guideline AQG 324 (2021), Chap. 8.2, p. 37.

[7] Keisuke Wakamoto, Yo Mochizuki, Takukazu Otsuka, Ken Nakahara and Takahiro Namazu "Tensile mechanical properties of sintered porous silver films and their dependence on porosity," Japanese journal of Applied Physics, vol. 58, no. SD, pp. SDDL08-1-5,2019,doi: 10.7567/1347-4065/ab0491.